Carbohydrate Research 543 (2024) 109216

Contents lists available at ScienceDirect

Carbohydrate Research

journal homepage: www.elsevier.com/locate/carres

Synthesis of hydrogels from biomaterials and their potential application in tissue engineering

Gabriela Martínez-Mejía [a], Ricardo Cuadras-Arconada [b], Nadia Adriana Vázquez-Torres [c], Rubén Caro-Briones [a,d], Andrés Castell-Rodríguez [c], José Manuel del Río [e], Mónica Corea [a,*], Rogelio Jiménez-Juárez [b,**]

[a] Laboratorio de Investigación en Polímeros y Nanomateriales, Instituto Politécnico Nacional, UPALM, Escuela Superior de Ingeniería Química e Industrias Extractivas, Edificio Z-5, PB, San Pedro Zacatenco, Alcaldía Gustavo A. Madero, CP 07738, Ciudad de México, Mexico
[b] Departamento de Química Orgánica, Instituto Politécnico Nacional, Escuela Nacional de Ciencias Biológicas, Prolongación de Carpio y Plan de Ayala s/n, Alcaldía Miguel Hidalgo, CP 11340, Ciudad de México, Mexico
[c] Departamento de Biología Celular y Tisular, Universidad Nacional Autónoma de México, Facultad de Medicina, Circuito Interior, Ciudad Universitaria, Av. Universidad3000, C.P. 04510, Ciudad de México, Mexico
[d] Departamento de Mecánica, Instituto Politécnico Nacional, Escuela Superior de Ingeniería Mecánica y Eléctrica, UPALM, San Pedro Zacatenco, Alcaldía Gustavo A. Madero, CP 07738, Ciudad de México, Mexico
[e] Departamento de Metalurgia y Materiales, Instituto Politécnico Nacional, Escuela Superior de Ingeniería Química e Industrias Extractivas, UPALM, San Pedro Zacatenco, Alcaldía Gustavo A. Madero, CP 07738, Ciudad de México, Mexico

A B S T R A C T

In this study, a series of hydrogels were synthesized from chitosan(s) that was crosslinking with glutaraldehyde at different concentrations. Ascorbic acid in an acidic medium was used to facilitate non-covalent interactions. The chitosan(s) was obtained from shrimp cytoskeleton; while ascorbic acid was extracted from xoconostle juice. The hydrogel reaction was monitored by UV–vis spectroscopy (550 nm) to determine the reaction kinetics and reaction order at 60 °C. The hydrogels structures were characterized by NMR, FT-IR, HR-MS and SEM, while the degree of cross-linking was examined with TGA-DA. The extracellular matrices were obtained as stable hydrogels where reached maximum crosslinking was of 7 %, independent of glutaraldehyde quantity added. The rheological properties showed a behavior of weak gels and a dependence of crosslinking agent concentration on strength at different temperatures. The cytotoxicity assay showed that the gels had no adverse effects on cellular growth for all concentrations of glutaraldehyde.

1. Introduction

Chitin is considered the second most abundant polysaccharide, just below cellulose. Monika Yadav et al. [1] and Michel Cauchie et al. [2] reported in 2019 that the annual production of chitin by freshwater arthropods was 280 million tons, while athalassohaline ecosystems were 6 million tons, and for marine ecosystems 1328 million tons. On the other hand, Núñez-Gómez and co-workers reported that the quantity of shrimp waste was of 20 tons in 2003 and the annual production of chitin alone is about of 170 thousand tons [3]. On the other hand, shrimp shell contains about 30–50 % minerals matter, 30–40 proteins and 20–30 % chitin. Furthermore, it is known that around 60 % of whole shrimp is by-products (head and hard carapace) after processing [4]. Almost all of shrimp waste is burned or thrown in the garbage on the beaches causing problems of environmental pollution and odors problems by the bacterial decomposition of shrimp waste [5].

However, seafood waste has high added-value polysaccharides, as chitin, proteins, free amino acid, carotenoid pigments, unsaturated fatty acids, flavours, enzymes, animal nutrition, remotion of metallic ions, dyes, and organic solvents that can be isolated by chemical and biochemical methods [6–15]. Specifically, chitin and its deacetylated form chitosan(s) display a wide range of applications, e.g., in food, cosmetics, agriculture, medical, biomedical and paper industry, among others [16–20].

It is well known that chitosan(s) has properties of biodegradability, biocompatibility, low immunogenicity, non-toxicity and antimicrobial action [21,22].For this reason, it can be used in the synthesis of extracellular matrices which provides a structural scaffold by means of a network of interactions. These interactions are involved in the formation of supramolecular assemblies and in cell-matrix interactions that

* Corresponding author.
** Corresponding author.
E-mail addresses: mcoreat@yahoo.com.mx (M. Corea), rjimenezj@ipn.mx (R. Jiménez-Juárez).

https://doi.org/10.1016/j.carres.2024.109216
Received 28 November 2023; Received in revised form 8 July 2024; Accepted 11 July 2024
Available online 15 July 2024
0008-6215/

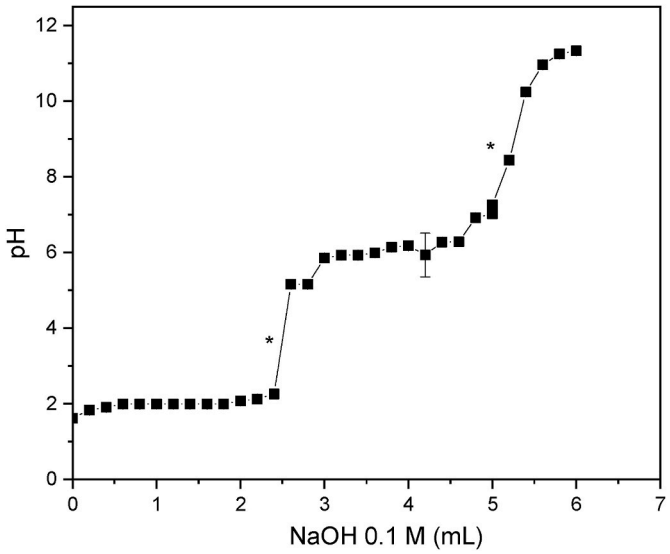

Fig. 1. Chitosan potentiometric titration.

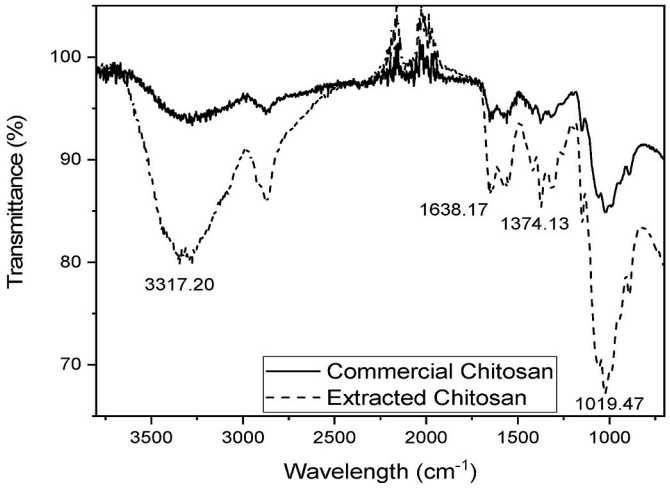

Fig. 2. Comparison between spectrum FT-IR of commercial and extracted chitosan(s).

regulate cell growth and behavior [23]. Therefore, the synthetic extracellular matrices (SECM) have some similarities to the natural extracellular matrices and try to mimic their biological activity. For this reason, they could have potential applications in regenerative medicine [24–26].

A disadvantage of chitosan(s) is only soluble under acidic conditions and its gels have poor mechanical properties. Therefore, chitosan(s) is required to be cross-linked by physical and/or chemical methods to improve its the mechanical properties, degree porosity, water absorbing capacity, permeation ability, among others [27–29].

The chitosan(s) can be crosslinked by means of physical interactions or chemical reactions using different cross-linking agents. For example, El-Dib and co-workers [30] synthesized cross-linked hydrogels able to absorb high quantity of water and other fluids. These gels were made first coupling chitosan(s) (CS) with maleic anhydride (MA) to obtain cross-linker N-maleyl chitosan(s) (N-MACS). After that, the obtained gels were crosslinked with acrylic acid (AA) and acrylamide (AM) using ammonium persulfate as catalyst in basic medium for to obtain N-maleyl poly(acrylic acid-*co*-acrylamide (NMACH P(AA-*co*-AM). In the same way, Johana Galan and co-workers [30] cross-linked chitosan(s) with glutaraldehyde and evaluated its ability to remove anionic dyes from industry wastewater. On the other hand, Minji Kim and co-workers [31] coupled chitosan(s) and hyaluronic acid through of 4-hydroxyphenylacetic acid promoting the reaction with *Streptomyces avermitilis-derived tyrosinase* with the purpose of encapsulating the Pancreatic-β cells for type 1 diabetes therapy. Another example, it is the work developed by Veino Risto Shaumbwa and co-workers [32]. They built magnetic chitosan(s) combining metal oxides as magnetite (Fe_3O_4) and evaluated its potential application to remove heavy metal ions from wastewater. Likewise, Yaping Wang et al. [33] made to react functionalized anionic aldehyde, hyaluronic acid-cationic and hydroxyethyl chitosan(s) with the purpose to be applied in therapy of breast cancer. On the other hand, Fatemeh Doustdar et al. [34] synthesized a physical scaffold of chitosan (s) and cellulose using calcium chloride as crosslinking agent. The prepared scaffold was used to release a curcumin drug. Gerald Draeger et al. [35] applied the Click reaction between the chitosan(s) and oxanorbornadiene derivatives by under metal free strategy, while Barreiro and Santameria-Echart and co-workers [36] made crosslinked chitosan (s) microspheres by means of physical interactions and chemical bonds. For that, sodium tripolyphosphate was used as physical cross-linking agent and vanillin as chemical cross-linking agent with the purpose to encapsulate active principles, gases and compounds with bad odors. An ingenious proposal was made by Mohammed Elhag et al. [37] who cross-linked chitosan(s) with ethyl 5-(2,5-dihydroxy-1,4-dioxan-2-yl)-2-methylfuran-3-carboxylate and its anti-proliferative activity was evaluated. In case of bone tissue engineering, Jue Hu et al. [38] built a scaffold from chitosan(s)-vanillin-bioglass through of physical and chemical phenomena which had good potential application in the tissue repair.

In this work, the synthesis of hydrogels by non-covalent intermolecular interactions between chitosan(s) (CS) previously extracted of shrimp cytoskeleton and ascorbic acid is reported. The ascorbic acid was extracted from xoconostle juice which comes from a natural source, instead of acetic acid using in the synthesis of SEMC reported in previous works [39].

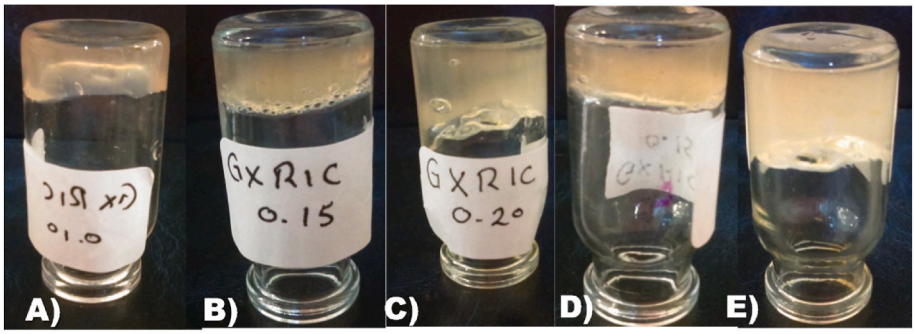

Fig. 3. Photographs of hydrogels of chitosan(s)-xoconostle juice and different concentrations of glutaraldehyde: A) 4 wt%; B) 6 wt%; C) 8 wt%; D) 10 wt%; E) 12 wt%.

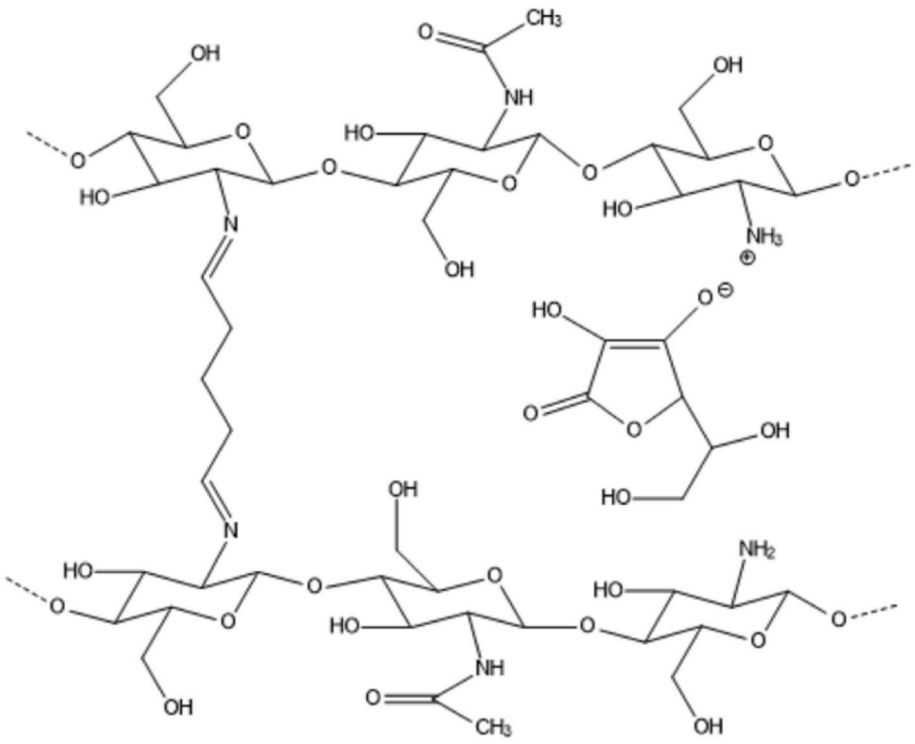

Fig. 4. Synthetic extracellular matrices formed by physical and chemical intermolecular covalent and non-covalent interactions, between chitosan(s), glutaraldehyde and ascorbic acid from xoconostle juice.

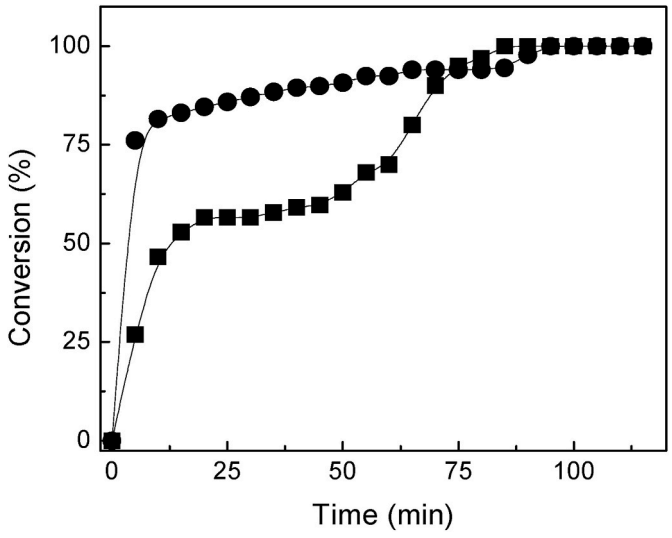

Fig. 5. Glutaraldehyde conversion as a function of time for the hydrogels with 4 wt % (●) and 10 wt % (■).

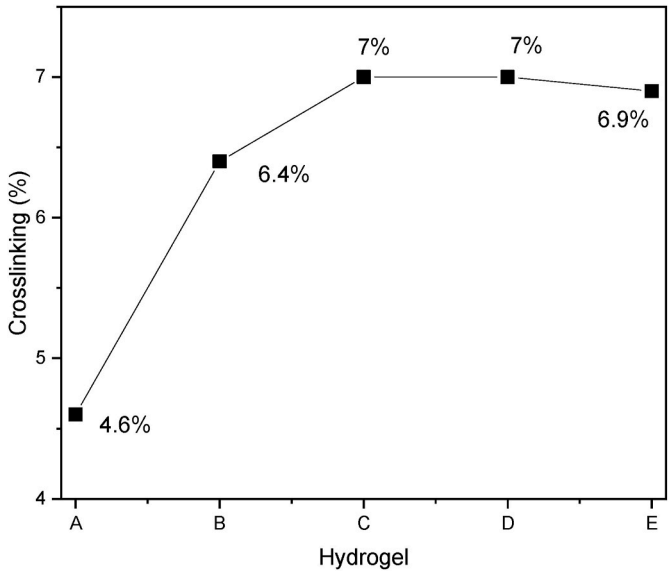

Fig. 6. Crosslinking percentage of hydrogels.

Xoconostle fruit (Opuntia xoconostle F. A. C. Weber ex Diguet, cv Cuaresmeño) grows in arid and semi-arid climates and is used as a condiment in the Mexican cuisine and for preparation of candies, jellies, beverages, gravy, among others. The fruit has three parts: the epicarp (the skin), the mesocarp (pulp) and the endocarp (where the seeds are tightly packed together in a mucilaginous structure). Despite being a fruit widely used in different food areas, it is sometimes considered a waste food, so this work proposes to take advantage of the fact that xoconostle juice contains ascorbic acid that can be used as a physical crosslinking agent for hydrogels [40]. It is important to mention, it is the first time that the xoconostle is used as physical crosslinking agent in the synthesis of hydrogels. The mesocarp is the edible part and contains high concentration of ascorbic acid 20.63 ± 0.32 mg/100g fresh weight [41, 42].

The obtained hydrogels in this work were characterized by Fourier-transform infrared spectroscopy (FT-IR), scanning electron microscopy (SEM) and thermogravimetry (TGA). The degree of cross-linking of the hydrogels was determined by Soxhlet techniques and the rheological properties such as loss and storage modulus were measured to determine the gel strength. Finally, the cellular viability and cytotoxicity of obtained materials were also evaluated with Human Mesenchymal stem cells (MSCs).

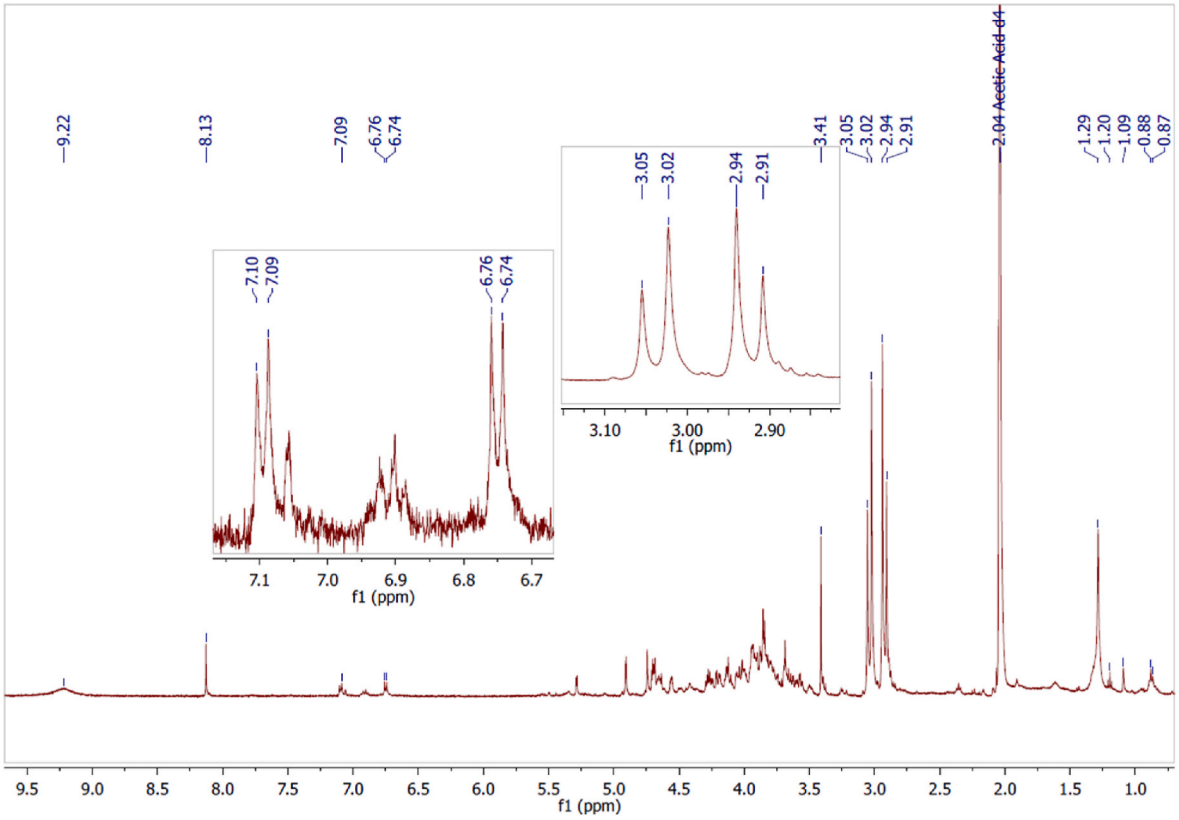

Fig. 7. NMR spectra of chitosan(s) extracted.

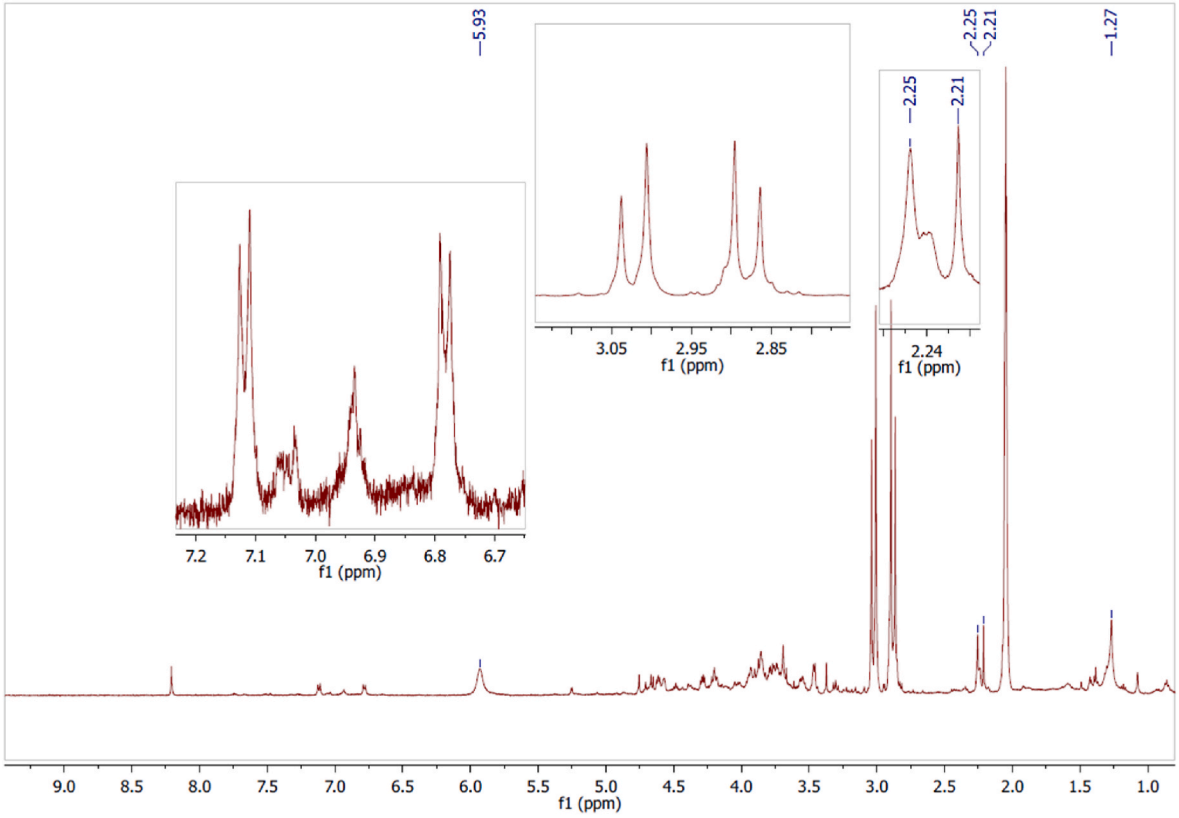

Fig. 8. NMR spectra of hydrogel at 4 wt%.

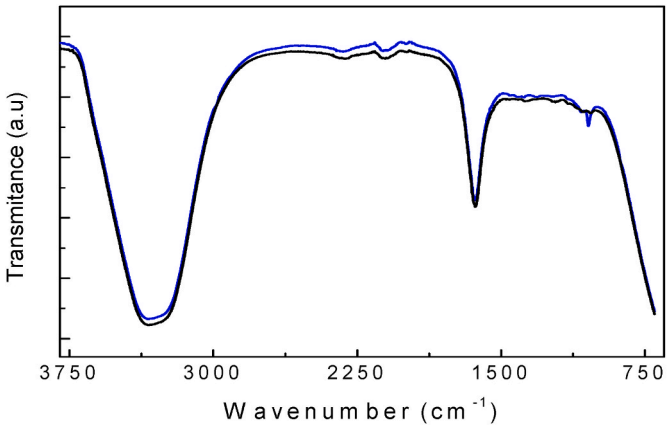

Fig. 9. FT-IR of hydrogels: 4 wt.% (—) and 12 wt. % (—) with crosslinking agent.

2. Materials and methods

2.1. Materials

The used chitosan(s) was obtained from the shrimp cytoskeleton. Purchased chitosan(s) and 2,4-dinitrophenylhydrazine (99 %) obtained from Sigma-Aldrich (Iceland), ethyl acetate, methylene chloride from Sigma Aldrich (USA), hexane (99 %), ethanol (99 %) and acetone (99 %) from Alveg (Mexico), and glutaraldehyde (25 wt%) from Merck (Germany). Distilled water grade II was used as solvent and xoconostle (Opuntia joconostle) from Teotihuacan Mexico was used as reaction media.

2.2. Methods

2.2.1. Extraction of chitosan(s)

The used chitosan(s) was obtained from the shrimp cytoskeleton. For that, 50 g of shredded cytoskeleton was added to 400 mL of sodium hydroxide solution (5 wt%) and they were heated at 60 °C during 2 h. The resulting suspension was filtered and washed with water until neutral pH. The product was dried at 75 °C. After that, the material was treated with 50 mL HCl (1 M; 1:3) at room temperature. The mixture was stirred by 30 min. The obtained suspension was filtered and washed with water until neutral pH. The obtained solid was dried at 75 °C. The obtained chitin was de-acetylated with 1 L NaOH solution (50 wt/v%); 1:3 at 90 °C and stirred during 1 h. The obtained chitosan(s) was washed with distilled water until neutral pH and was dried at 75 °C and its melting point was determined by melting point apparatus Electrothermal FQI-136.

2.2.2. Potentiometric titration

To determinate the degree of deacetylation, chitosan(s) samples (0.05 g) was dissolved in a 1 % acetic acid solution. This solution was titrated with a 0.1 M NaOH solution, measuring pH with a pH-meter CONDUCTRONIC PC 45. Potentriometric tritations were made by triplicate.

2.2.3. Preparation of xoconostle juice

The xoconostle juice was used as reaction media because to its high content of ascorbic acid. For that, the shell and seeds of cactus were removed. The obtained pulp was cut in pieces of 2 cm and, 500 g of it was washed with 500 mL of hexane during 4 h. After that, the mixture was suspended with 200 mL of distiller water and filtered to obtain the xoconostle juice.

2.2.4. Preparation of hydrogel

The hydrogels were prepared with 0.03 g of chitosan(s) and 1.5 g of xoconostle juice. The mixture was stirred and heated at 60 °C. Different aliquots (0.05, 0.1, 0.15, 0.20 and 0.25 mL) of glutaraldehyde (1.25 % aqueous solution) were added dropwise and the reaction mixture was stirred during 1 h at room temperature. The obtained viscous solution was cooled in an ice-water bath between 0 and 2 °C to form the hydrogel.

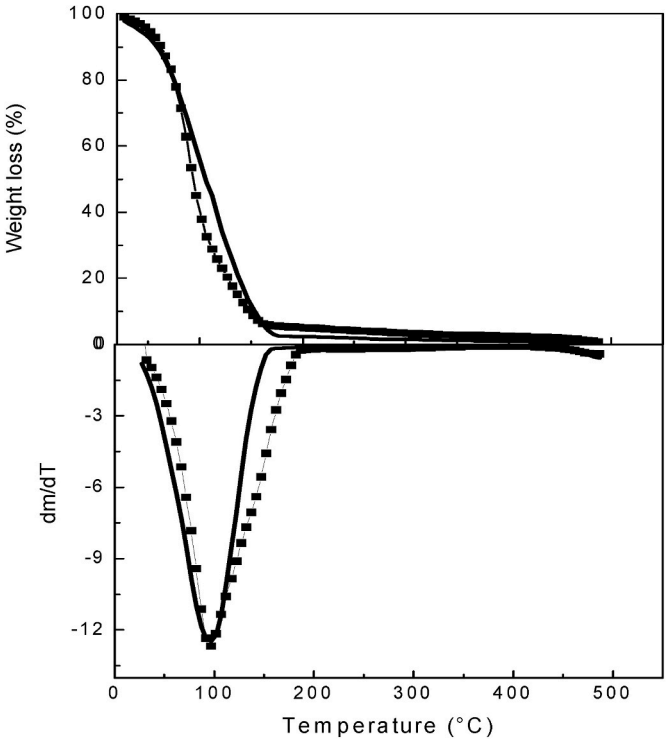

Fig. 11. Thermogravimetric analysis of hydrogels with 4 (▬) and 10 (■) wt % of glutaraldehyde.

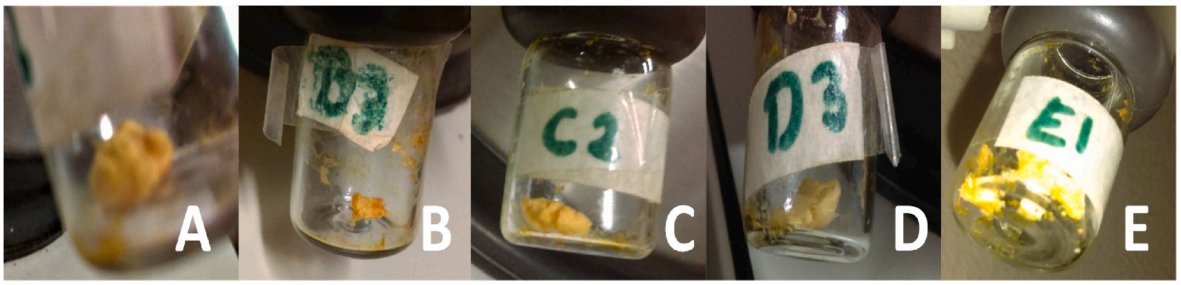

Fig. 10. Freeze-drying of hydrogels with 4, 6, 8, 10 and 12 wt% of crosslinking agent.

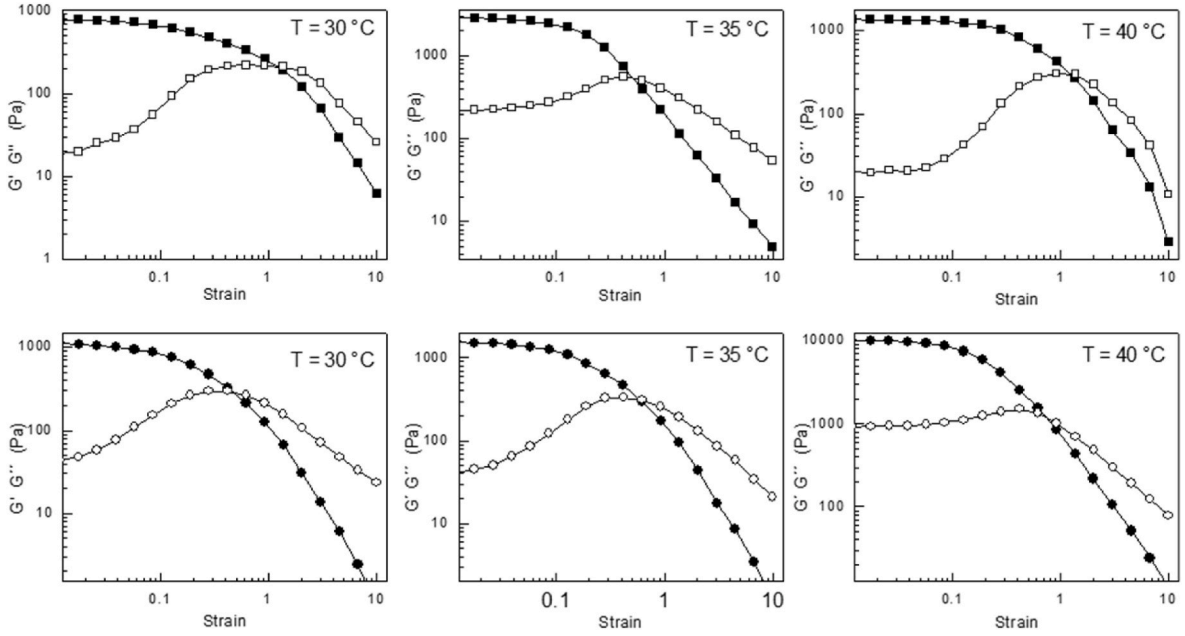

Fig. 12. Dynamic strain sweep analysis of hydrogels with 4 wt % (■) and 10 wt % (●) of glutaraldehyde. G′ (solid symbols) and G″ (open symbols).

2.2.5. Determination of the reaction conversion between chitosan(s) and glutaraldehyde

The method to determine the reaction conversion has been reported in a previous work [41]. Briefly, the reaction between chitosan(s) and glutaraldehyde was monitored by UV–vis spectroscopy at 550 nm in a PerkinElmer Lamda 25 UV–vis double beam spectrophotometer (Model 643, USA), 0.5 g samples every 5 min. Samples were extracted with 2 mL of methylene chloride under vigorous agitation and then, 2 mL of ethanol and 2 mL 2,4-dinitrophenylhydrazine of acid alcoholic solution (DNP) were added to the organic phase and the mixture was stirred. The samples were analyzed by UV–vis spectroscopy and the glutaraldehyde conversion was determined.

2.2.6. Freeze-drying

The obtained hydrogels were freeze-dried in stages in a Labconco (S/M Series FJMJ98, USA) lyophilizer. For that, 1.5 g of each SECM sample was taken to first freezing step took place at 10 °C for 30 min. Afterwards, a vacuum of up to 89 × 10^{-3} mBars was applied and the second thermal stage of −46 ± 0.1 °C lasted 1.5 h. Finally, the temperature was elevated to 30 ± 0.1 °C and maintained for 1.5 h.

2.2.7. NMR studies

One-dimensional (1D) ^{1}H NMR spectra were recorded at 499.85 MHz on a Varian (now Agilent) NMR System 500 spectrometer (Agilent Technologies, Inc., Santa Clara, CA, USA). Samples of 30 mg of chitosan (s) extracted and a 30 mg of hydrogel with GA at 4 wt% were dissolved in deuterated acetic acid. As a reference for the ^{1}H NMR chemical shifts, the signals of non-deuterated solvent residues were set at $\delta = 2.04$ ppm for acetic.

2.2.8. FT-IR analysis

The hydrogel samples were analyzed by FT-IR on a PerkinElmer infrared spectrophotometer (Model 720 X, USA) using a double beam. The apparatus was equipped with attenuated total reflectance ATR reflectance Ge accessory PerkinElmer, model Frontier with energy of 176 U E (Waltham MA, USA). Spectra of the samples were recorded in transmission mode over the near infrared spectroscopy region between of 400–4000 cm^{-1}. Samples were weighed around 0.05g and scanned 4 times at 30 °C.

2.2.9. Mass spectroscopy analysis

Fresh hydrogel samples were examined by high-resolution mass spectrometry (HR-MS) on a mass spectrophotometer with micrOTOF II-Q and electrospray ionization (BrukerDaltonisc, Billerica, MA, USA).

2.2.10. Degree of crosslinking analysis

Briefly, 1.5 g hydrogel samples were washed with ethyl acetate. The degree of crosslinking (*D*) of the insoluble part of hydrogel was calculated gravimetrically by means of equation:(1)

$$\%D = \frac{W_g}{W_0} \text{x} 100 \quad (1)$$

where W_g is the sample weight after the wash and W_0 is the initial mass [39].

2.2.11. Thermogravimetric analysis

Derivate thermogravimetric analysis (DA-TGA) of the hydrogels was carried out on a 6000 PerkinElmer simultaneous thermal analyzer (Germany). A 0.5 g sample was heated from 25 to 500 °C at a rate of 10 °C/min under nitrogen atmosphere.

2.2.12. Rheological properties analysis

Rheological properties were evaluated with a Modular Compact Rheometer (model MCR 502, Anton Paar, Austria) using PP25 parallel plate geometry (25 mm diameter, 0°). A sample of 1.5 g was placed in the center of the bottom plate. The upper plate was immediately lowered to a gap of 1 mm and the measure was performed. The analysis was made at 30, 35 and 40 °C. The set of experiments were determinate by performing a shear strain (γ) range from 0.01 to 10 %, a range of frequencies from 100 to 0.1 rad/s and an angular velocity (ω) at 10 rad/s. The rheological properties were measured to determine the flow behavior of hydrogels and linear viscoelastic range, the measurements were made at 30, 35 y 40 °C.

2.2.13. Scanning electron microscopy (SEM) analysis

Surface morphologies and crosslinking sections of the CS scaffolds were frozen with liquid nitrogen and a vacuum was applied for 24 h. Subsequently, they were covered with gold and observed on a JEOL JSM 6400 field-emission scanning electron microscope (USA) at 5 kV.

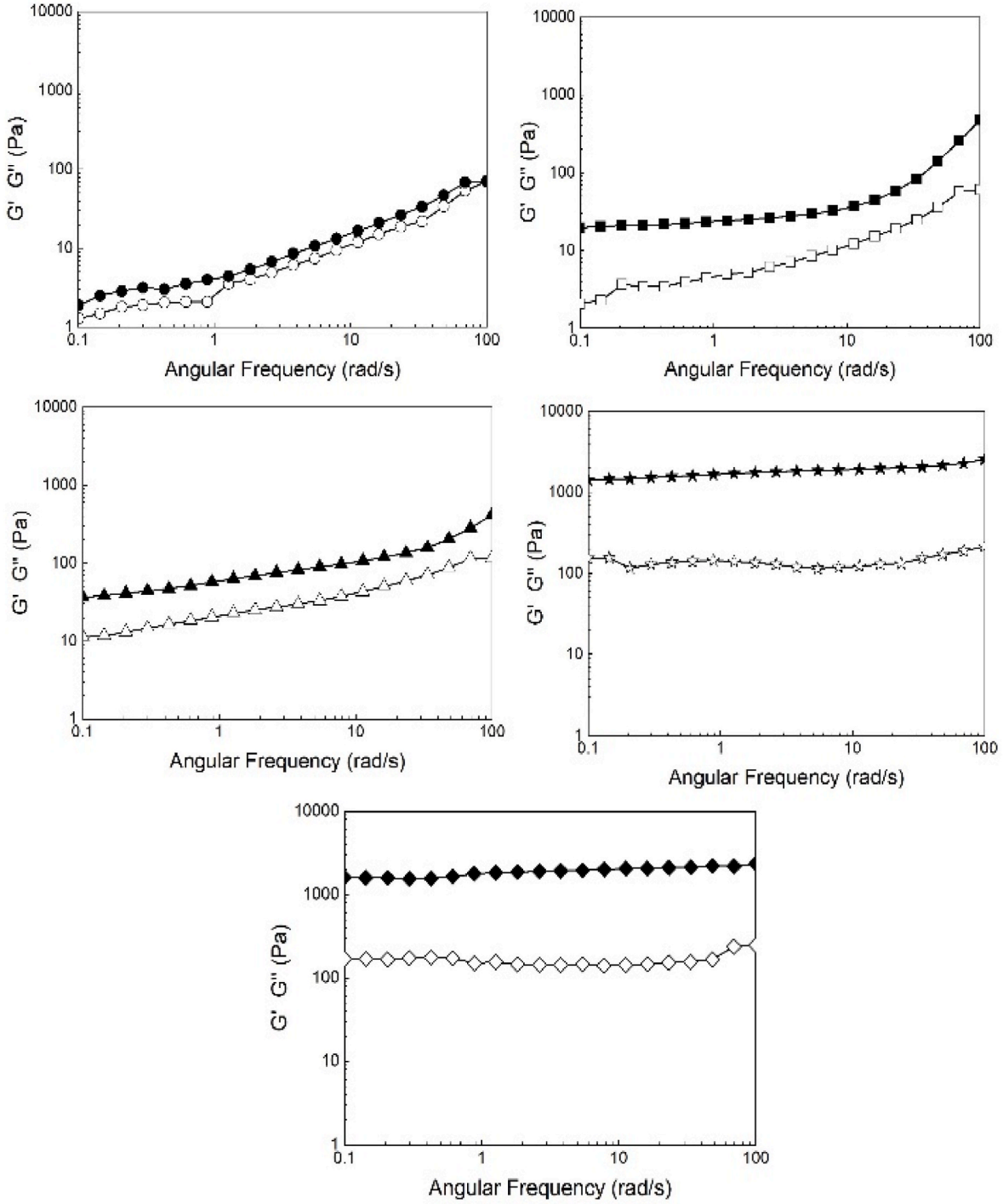

Fig. 13. Frequency sweep analysis of hydrogels with 4 wt.% (=), 6 wt. % (n), 8 wt.% (p), 10 wt.%(ê) and 12 wt.% (¿) of glutaraldehyde. G′ (solid symbols) and G″ (open symbols).

2.2.14. Cytotoxicity assay analysis

The cytotoxicity and viability tests were made with Human Mesenchymal stem cells (MSCs) which were isolated from Wharton's jelly explants. The explants were cultured in DMEM-F12 medium supplemented with 10 % FBS and 1 % penicillin-streptomycin at 37 °C and 5 % CO_2. The culture medium was replaced every 2 days and after 2 weeks of culture, the explants were removed. MSCs were cultured until reaching approximately 80 % confluence, and the cells were detached with 0.05 %/0.02 % trypsin/EDTA.

Thin layers samples of gels were put on 0.5 × 0.5 mm coverslip frames and were put in 48-well plates and sterilized by UV irradiation and washes with ethanol (70 %). Subsequently, 10 μL of cell suspension in DMEM-F12 was seeded onto gels samples (10,000 cells per sample) and incubated for 1 h at 37 °C. Finally, 500 μL of DMEM-F12 were added to the gels and they were maintained at standard culture conditions.

After 3 days, the viability of MSCs was evaluated with a live/dead viability -cytotoxicity kit for mammalian cells (Thermo Fisher Scientific, Canada). The cell-seeded gels were rinsed with PBS solution and incubated with Calcein AM and ethidium homodimer solution for 1 h at 37 °C. Live cells were stained green with calcein, while the nuclei of dead

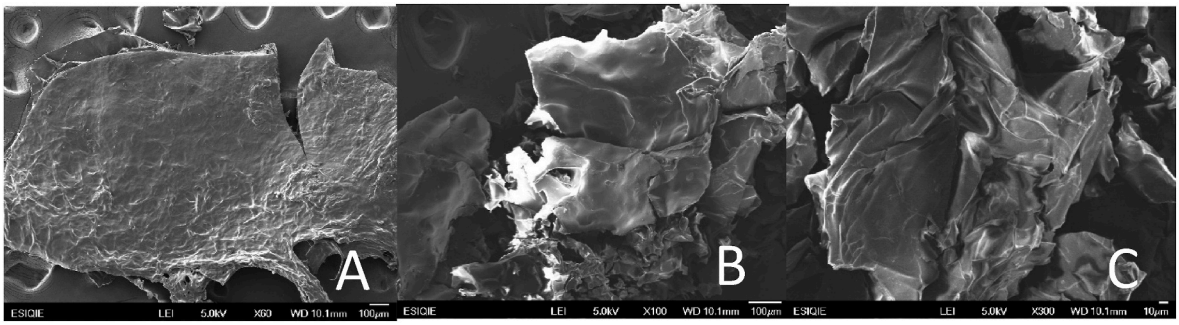

Fig. 14. Microscopy images of the surfaces of scaffolds lyophilized containing 4 wt%(A), 8 wt%(B) and 12 wt%(C) of the crosslinking agent.

cells is red, thus providing the basis of the fluorescence live/dead assay. In addition, the MSC viability the overall cell morphology was observed by epifluorescence microscopy (Nikon Eclipse 80i, Tokio Japan).

3. Results and discussion

3.1. Chitosan(s) extraction

The chitosan(s) was extracted from the shrimp cytoskeleton and it was obtained as a beige solid with a weight of 38 g (75 % yield) and a melting point of 103.4 °C, corresponding to a chitosan with an average molecular weight of 170 kDa [43].

3.2. Potentiometric titration

The degree of deacetylation of chitosan(s) was determined by acid-base titration with a 0.1 M NaOH solution. The variation of the pH of the chitosan(s) solution was plotted as a function of the added volume of NaOH. The titration curve (Fig. 1) was obtained, where two equivalent points could be distinguished. The first point at 2.5 mL of NaOH added, which corresponds to the neutralization of excess acetic acid ($H^+ + OH^- \rightarrow H_2O$). The second point at 5.4 mL attributed to the protonation of the amine groups of the glcosamine residues of chitosan. At acidic pH, the primary amino groups are protonated, and upon addition of NaOH during titration, they are neutralized ($-NH_3^+ + OH^- \rightarrow -NH_2 + H_2O$) and, therefore, their concentration can be quantified [44].

The degree of deacetylation (*DD*) was calculated from the following equation proposed by Perez et al.

$$DD = 161\left(10^{-3}\right)(y - x)\left(\frac{M}{w}\right)$$

where 161 is the molar mass of the monomeric unit of fully deacetylated chitosan(s) (g mol^{-1}), *y* and *x* are the second and first equivalent points (mL), respectively, M is the concentration of the NaOH solution (mol L^{-1}) and w is the weight of chitosan(s) (g) [44]. The obtained *DD* value was 93.38 %.

3.3. Chitosan(s) extraction FT-IR

The chitosan(s) was analyzed by FT-IR and compared with the purchased chitosan (s) (Fig. 2). The spectrum of extracted chitosan(s) shows a wide band at 3317.20 cm^{-1} corresponding to OH and other at 1638.17 cm^{-1} of the carbonyl, characteristic of acetamide groups ($HN–COCH_3$) belonging of chitosan(s). The FT-IR results were confirmed with the spectrum of purchased chitosan(s), where these bands appear at the same wavenumber.

3.4. Hydrogel synthesis

Xoconostle juice was obtained as an opaque rose liquid with a volume of 250 mL with 50 % yield. A series of extracellular matrices were prepared with the extracted chitosan(s), xoconoxtle juice (as the ascorbic acid medium) and glutaraldehyde. The samples were synthesized by triplicate. The glutaraldehyde was used as crosslinking agent and its concentration was changed between 4, 6, 8, 10 and 12 wt%. Fig. 3 shows the photographs of obtained materials. It can be observed that all hydrogels have a slight salmon color characteristic of xoconoxtle juice. The photographs show that all the materials were stable because they do not present runoff and lumps in their structure; except the hydrogel with 4 wt% of glutaraldehyde (A). This could be attributed to the quantity of crosslinking agent is not sufficient to form a good gel.

A possible scheme of gel formation is shown in Fig. 4, The formation of three-dimensional network inside the hydrogel is due to covalent bonds between chitosan(s) and glutaraldehyde and non-covalent interactions between chitosan(s) and ascorbic acid. In addition, it has reported that the amino groups of chitosan(s) are protonatable in the acidic media, whereas the acidic hydroxyl groups of ascorbic acid allow the ionic interaction [45].

3.5. Hydrogel reaction kinetics

The conversion of glutaraldehyde as a function of time was followed according of a method reported in a previous work [41], to understand the synthesis of hydrogels where, a sample of reaction was taken every 5 min and a quantity of DNP was added to form a yellow complex color with the unreacted glutaraldehyde. The obtained sample was measured in a Uv–vis instrument at 553 nm. The obtained result was compared with a calibration curve previously built. The conversion results of hydrogels with 4 and 10 wt% of crosslinking agent as a function of time are shown in Fig. 5 as an example, because these concentrations glutaraldehyde were considered as the extreme values. The plot shows that the materials with 4 wt% almost reach a 50 % of conversion during the first 12 min of reaction. After this point, the glutaraldehyde conversion is slow, while the materials with 10 wt% had a conversion of 80 % at the first 5 min and the complete conversion was reached after 100 min. This behavior was the slower, if these results are compared with those reported in a previous work [41] where the hydrogels of chitosan (s) and glutaraldehyde were synthesized in presence of acetic acid. This behavior could be attributed to gels made with xoconostle juice do not allow the diffusion of glutaraldehyde inside of hydrogel at high conversions, decreasing the crosslinking reaction rate. Other explanation is that may be the carbonyl group of the amide could had been arrested for non-covalent interactions with the ascorbic acid. For this reason, the used glutaraldehyde as crosslinking agent was not consumed totally.

3.6. Hydrogel crosslinking degree

The crosslinking degree was obtained for every hydrogel using a Soxhlet system. The materials were washed with ethyl acetate and the insoluble part (crosslinked polymer) was separated and weighted. After that, the crosslinking percentage was calculated using equation (1). The obtained results are shown in Fig. 6. It is observed that the materials

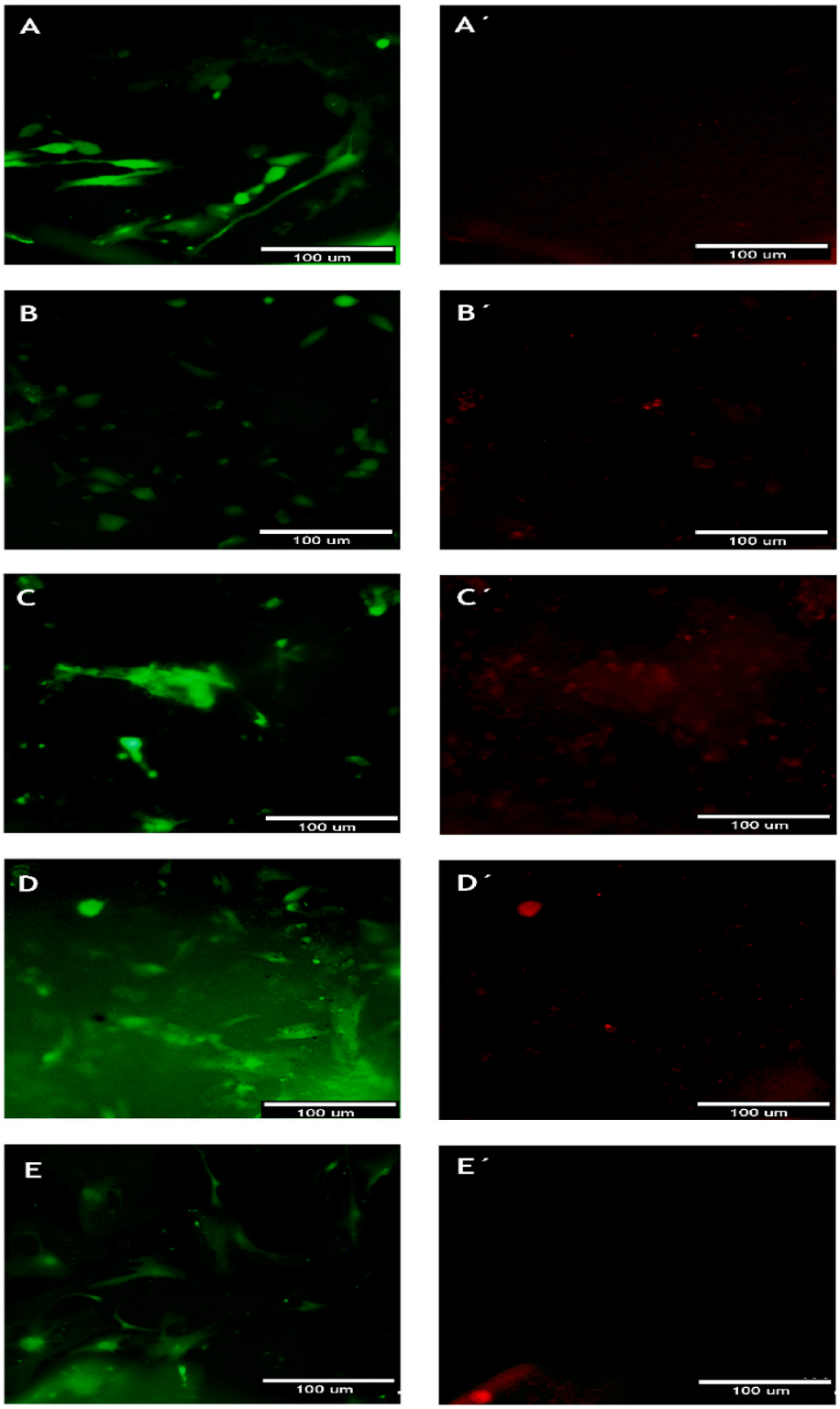

Fig. 15. Fluorescence micrographs of fibroblast cells onto hydrogels with the crosslinking agent at 4 wt% (A), 6 wt% (B), 8 wt% (C), 10 wt% (D) and 12 wt% (E). Live cells are visible as green, dead cells are observed as red.

reached a maximum value of crosslinking of 7 %. This value was independent of quantity of glutaraldehyde added. This same behavior is presented for the hydrogels with 8, 10 and 12 wt% which confirms the obtained results in the conversion curves and attributed to the composition of xoconostle juice [41].

3.7. NMR studies

The ^{1}H NMR spectrum of the extracted chitosan(s) (Fig. 7) showed a quadruplet around $\delta = 3.00$ ppm, multiple signals at $\delta = 4.00$ ppm corresponding to CS. These signals are also coincided with the spectrum of pure glucosamine as well as bibliographical data.

The ^{1}H NMR spectrum of the hydrogel crosslinking at 4 wt% were

presented in Fig. 8. It showed the same signals of chitosan(s) and the appearance of a signal in $\delta = 5.00$ ppm attributed at presence of ascorbic acid (O–C–H) of xoconostle juice.

3.8. Hydrogel FT-IR

The hydrogels were analyzed by FT-IR to confirm the crosslinking degree. Fig. 9 shows the spectra of gels synthesized with xoconostle with 4 and 12 wt % of glutaraldehyde as an example, because all the materials have the same shape. In both cases, a band attributed to the imine is observed at 1635 cm^{-1} because the crosslinking reaction between chitosan(s) and glutaraldehyde. In addition, there is not bigger difference in the absorption intensity when the crosslinking agent concentration is increased. This could be attributed to a limit in the crosslinking reaction when is carried out in presence of xoconoxtle juice as reaction medium, because the chitosan(s) and ascorbic acid from xoconoxtle form a salt and anchor the hydrogel [46]. This could explain why there is no change in the absorption band at 1635 cm^{-1} when the glutaraldehyde concentration is increased and confirms the obtained results of swelling degree.

3.9. Freeze-dried hydrogel

The hydrogels were also freeze-dried in stages. For that, a sample was taken and freezing at 10 °C. Afterwards, a vacuum was applied, and temperature was lowered at -46 ± 0.1 °C. Finally, the temperature was elevated to 30 ± 0.1 °C. Fig. 10 shows the photographs hydrogels freeze-dried. It is observed that all obtained materials presented a light-yellow color and their appearance is as a sponge with a cork type texture, where the porosities are by the sublimation water contained into the gels before the treatment.

3.10. Hydrogel thermogravimetric

The fresh hydrogels were also analyzed by thermogravimetric techniques. Fig. 11 presents the results of hydrogels with xoconostle with 4 and 10 wt% of glutaraldehyde. The thermogram for both samples show a first weight loss at temperatures close to 50 °C attributed to the loss of contained water into the sample. After that, there is a continues weight loss until reach the total decomposition of material which is observed at 150 °C for the hydrogels with 4 wt% of glutaraldehyde, while for the material with 10 wt% of crosslinking agent this decomposition point was observed at temperature close to 178 °C. This difference is attributed to the quantity of crosslinked chains for each sample. For other hand, the bibliography has been reported decomposition temperatures of chitosan (s)-glutaraldehyde up 200 °C. This behavior could be attributed first to the crosslinked degree of materials, because the concentration of glutaraldehyde these works are higher than those obtained in this work. Second the average molecular weight of obtained chitosan(s) for this work could be lower than those reported by bibliography, because it was extracted from the shrimp cytoskeleton in the laboratory [46,47].

3.11. Rheological properties

The rheological properties were measured to determine the flow behavior of hydrogels and linear viscoelastic range, the measurements were made at 30, 35 y 40 °C. The elastic modulus (G′) denoted by solid symbols and the viscous modulus (G″) marked with open symbols for hydrogels containing 4 % and 10 % of crosslinking agent are presented in Fig. 12, as example. Parameters include shear strain (γ) ranging from 0.01 to 10 % and angular velocity (ω) at 10 rad/s.

For clarity, it is important to note that G′ represents the energy stored during physical or shear stress (i.e. the solid phase of the hydrogel), while G″ corresponds to the dissipated energy during physical/shear stress (i.e. the liquid phase of the hydrogel). Across all cases, the results consistently indicate that G′ surpasses G″, affirming the prevailing elastic nature of these materials. Moreover, a rapid decrease in G′ at lower stresses is evident, characteristic of a weak gel behavior, as previously reported [46,47]. A dependence of crosslinking agent concentration on strength at different temperatures was also observed. For example, the hydrogel with 10 wt% of glutaraldehyde at 40 °C presented the higher modulus than the hydrogel with 4 wt% of crosslinking agent.

The frequency sweep analysis allows to evaluate the stability of gels. Short-term behavior is simulated by rapid motion (high frequencies) and long-term or rest behavior by slow motion (low frequencies). The elastic modulus (G′) as solid symbols and the viscous modulus (G″) as open symbols for all hydrogels across a range of frequencies from 100 to 0.1 rad/s are presented in Fig. 13. It is noteworthy that in all materials, the curves of G′ consistently exhibit higher values than the G″ curves. These curves also appear to form nearly parallel straight lines throughout the entire frequency range, showing only a slight slope. This behavior could define a consistency at rest and long-term storage stability in the material. With exception of the gels with 4 wt% of glutaraldehyde, all hydrogels present modulus above 10 Pa, denoting the gel stability [46].

Furthermore, by conducting this rheological test insights into the "rigidity" or the degree of crosslinking within the gels. Hydrogels with a higher degree of crosslinking will exhibit a correspondingly higher plateau value of G′ in the low-frequency range. An example of this, is observed in the hydrogels containing 12 wt% of glutaraldehyde.

3.11.1. Scanning electron microscopy (SEM) analysis

The morphology of freeze-dried hydrogels was examined by SEM. Micrographs of the hydrogels containing 4 wt% of crosslinking agent (Fig. 14A) show flat and corrugated surfaces while hydrogels containing 8 wt% (Figs. 14B) and 12 wt% (Fig. 14C) of the crosslinking agent show greater porosity, apparently because the lyophilization process.

3.12. Hydrogel cytotoxicity

The cytotoxicity of gels was evaluated using calcein and ethidium homodimer staining. For the viability assay. The esterase activity in alive cell was evaluated by fluorescence of calcein while the cell membrane permeability was evaluated with ethidium homodimer taking account that dead cells present a damaged membrane. The samples were observed in an epifluorescence microscope. The obtained images are shown in Fig. 15. The results show that the gels did not have effect on MSCs for all concentrations of glutaraldehyde, except to 8 wt% (Fig. 15C) where dead cells were observed (Fig. 15C). The viable cells were on the surface of gels, indicating that MSCs were attached to the biomaterials. A typical fusiform morphology of MSC in normal cell culture was observed. In addition, round morphology cell was appreciated in gels with 4, 6 and 8 wt % of glutaraldehyde.

4. Conclusions

A series of hydrogels from chitosan(s) extracted of shrimp cytoskeleton and glutaraldehyde in presence of xoconostle juice as source of ascorbic acid were synthesized. The yield of extracted chitosan(s) was 75 %. This was confirmed with FT-IR results, where are showed the same absorption bands that purchased chitosan(s). When the percentage of crosslinking agent in the hydrogels was quantified, the results showed that only the 7 wt % of glutaraldehyde was incorporated into the hydrogels, for theoretical crosslinking agent concentrations higher than 8 wt%. This was attributed to the formation of a salt between chitosan(s) and ascorbic acid from xoconostle, anchoring them to the polymeric hydrogel. This was also corroborated by FT-IR results. The rheological properties confirmed the weak gel formation and there is an influence of crosslinking agent in the strength of gel at 40 °C. The SEM images confirm highly porous structures. In addition, the viable cells were on the surface of gels, indicating that MSCs were attached to the biomaterials. According to the obtained results, the synthesized hydrogels could be considered promising biomaterials in regenerative medicine. Their ability to promote wound healing and their biocompatibility offer

significant advantages. However, it is crucial to address limitations such as the variability of physicochemical properties and the need to optimize stability and degradation. These challenges represent research opportunities to further boost their clinical application. Ultimately, the combination of the unique properties of these hydrogels could revolutionize the field of regenerative medicine, offering new solutions for the treatment of injuries and chronic diseases.

CRediT authorship contribution statement

Gabriela Martínez-Mejía: Writing – original draft, Methodology, Investigation, Formal analysis, Data curation. **Ricardo Cuadras-Arconada:** Methodology, Investigation, Formal analysis, Data curation. **Nadia Adriana Vázquez-Torres:** Methodology, Investigation, Formal analysis, Data curation. **Rubén Caro-Briones:** Methodology, Investigation, Formal analysis, Data curation. **Andrés Castell-Rodríguez:** Writing – review & editing, Writing – original draft, Validation, Supervision, Resources, Methodology, Investigation, Formal analysis. **José Manuel del Río:** Resources. **Mónica Corea:** Writing – review & editing, Writing – original draft, Validation, Supervision, Resources, Methodology, Investigation, Formal analysis, Data curation. **Rogelio Jiménez-Juárez:** Writing – review & editing, Writing – original draft, Validation, Supervision, Resources, Methodology, Investigation, Formal analysis, Data curation.

Declaration of competing interest

The authors declare that they have no conflict of interest.

Data availability

No data was used for the research described in the article.

Appendix A. Supplementary data

Supplementary data to this article can be found online at https://doi.org/10.1016/j.carres.2024.109216.

References

[1] Monika Yadav, Priynshi Goswami, Kunwar Paritosh, Manish Kumar, Nidhi Pareek, Vivekanand Vivekanand, Bioresources and Bioprocessing 6 (2019) 8, https://doi.org/10.1186/s40643-019-0243-y.

[2] Henry-michel Cauchie, Hydrobiologia 470 (2002) 63–96.

[3] Dàmaris Nùñez-Gòmez, Caroline Rodriguez, Flàvio R. Lapolli, Marìa A. Lobo-Recio, J. Polym. Environ. 29 (2021) 576–587, https://doi.org/10.1007/s10924-020-01887-5.

[4] Gurpreet Singh Dhillon, Surinder Kaur, Satinder Kaur Brar, Mausam Verma, Crit. Rev. Biotechnol. 33 (4) (2013) 379–403, https://doi.org/10.3109/07388551.2012.717217.

[5] S. Jouanneau, L. Recoules, M.J. Durand, A. Boukabache, V. Picot, Y. Primault, A. Lakel, M. Sengelin, B. Barillon, G. Thouand, Methods for assessing biochemical oxygen demand (BOD): a review, Water Res. 49 (2014) 62–82.

[6] Xiangzhao Mao, Na Guo, Jianan Sun, Changhu Xue, J. Clean. Prod. 143 (2017) 814–823, https://doi.org/10.1016/j.jclepro.2016.12.042.

[7] Assaâd Sila, Nadhem Sayari, Rafik Balti, Oscar Martinez-Alvarez, Naima Nedjar-Arroume, Nasri Moncef, Bougatef Ali, Food Chem. 148 (2014) 445–452, https://doi.org/10.1016/j.foodchem.2013.05.146.

[8] Hongcai Zhang, Sanyue Yun, Lingling Song, Yiwen Zhang, Yanyun Zhao, Int. J. Biol. Macromol. 96 (2017) 334–339, https://doi.org/10.1016/j.ijbiomac.2016.12.017.

[9] Fatemeh Sedaghat, Morteza Yousefzadi, Hojjat Toiserkani, Sohrab Najafipour, Int. J. Biol. Macromol. 104 (2017) 883–888, https://doi.org/10.1016/j.ijbiomac.2017.06.099.

[10] Prameela Kandra, Murali Mohan Challa, Hemalatha kalangi padma jyethi, Applied Microbiol Biothechnology 93 (2012) 17–29, https://doi.org/10.1007/s00253-011-3651-2.

[11] Priyatharini Ambigaipalan, Fereidoon Shahidi, J. Funct.Foods 34 (2017) 7–17, https://doi.org/10.1016/j.jff.2017.04.013.

[12] Pei Liu, Shanshan Liu, Na Guo, Xiangzhao Mao, Hong Lin, Changhu Xue, Dongzhi Wei, Biochem. Eng. J. 91 (2014) 10–15, https://doi.org/10.1016/j.bej.2014.07.004.

[13] Yongliang Liu, Ronge Xing, Haoyue Yang, Song Liu, Yukun Qin, Kecheng Li, Huahua Yu, Pencheng Li Professor, Int. J. Biol. Macromol. 148 (2020) 424–433, https://doi.org/10.1016/j.ijbiomac.2020.01.124.

[14] Leta Deressa Tolesa, Bhupender S. Gupta, Ming-jer lee, Int. J. Biol. Macromol. 130 (2019) 818–826, https://doi.org/10.1016/j.ijbiomac.2019.03.018.

[15] Munirah M. Al-Rouodi, Masudul Hassan, Zaid Moussa, Rami J. Obaid, Nahid Hasan Suman, Manfred H. Wagner, Sameer S.A. Natto, Saleh A. Ahmed, J. Saudi Chem. Soc. 26 (2022) 101561, https://doi.org/10.1016/j.jscs.2022.101561.

[16] J. Zoldners, T. Kiseleva, I. Kaiminsh, Carbohydrate Polym. 60 (2005) 215–218, https://doi.org/10.1016/j.carbpol.2005.01.013.

[17] Tuanny Santos Frantz, Bruna Silva de Farias, Victor Ramon Mendonça Leite, Felipe Kessler, Tito Roberto Sant, Anna Cadaval Jr., Luis Antonio de Almeida Pinto, J. Clean. Prod. 269 (2020) 122397, https://doi.org/10.1016/j.jclepro.2020.122397.

[18] Muhammad Shahzad Saleem, Muhammad Akbar Anjum, Safina Naz, Sajid Ali, Sajjad Hussain, Muhammad Azam, Hasan Sardar, Ghulam Khaliq, Ihsan Canan, Shaghef Ejaz, Int. J. Biol. Macromol. 189 (2021) 160–169, https://doi.org/10.1016/j.ijbiomac.2021.08.051.

[19] Jolleen Natalie I. Balitaan, Jui-Ming Yeh, Karen S. Santiago, Int. J. Biol. Macromol. 154 (2020) 1565–1575, https://doi.org/10.1016/j.ijbiomac.2019.11.041.

[20] X.L. Tian, D.F. Tian, Z.Y. Wang, F.K. Mo, Indian J. Pharmaceut. Sci. 71 (4) (2009) 371–376.

[21] Soibam Ngasotter, K.A. Martin Xavier, Maibam Malemngamba Meitei, David Waikhom, Madhulika, Jyotirmoy Pathak, Soibam Khogen Singh, Crustacean shell waste derived chitin and chitin nanomaterials for application in agriculture, food, and health – a review, Carbohydr. Polym. Technol. Appl. 6 (2023) 1003–1049.

[22] M. Shivashankar, B. kumar mandal, R. Yerappagari, V.P. Kumar, A review on chitosan-based hydrogels for the drug delivery System, Int. Res. J. Pharm. 2 (2011) 1–6.

[23] Beatrice Yue, Biology of the extracellular matrix: an overview, J. Glaucoma (2014. Oct-Nov. 2014) S20–S23.

[24] A. Hopf, D.J. Schaefer, D.F. Kalbermatten, R. Guzman, S. Madduri, Schwann cell-like cells: origen and usability for repair and regeneration of the peripheral and central nervous system, Cell 9 (2020) 1990 (31.

[25] C. Chabannon, J. Kuball, A. Bondanza, F. Dazzi, P. Pedrazzoli, A. Toubert, A. Ruggeri, K. Fleischhauer, C. Bonini, Hematopoietic stem cell transplantation in its 60s: a platform for cellular therapies, Sci. Transl. Med. 10 (10) (2018) eaap9630.

[26] V. Lionetti, C. Ventura, Regenerative medicine approach to repair the failing heart, Vascul. Phamaco 58 (2013), 159-l.163.

[27] X. Liu, Y. Zhang, H. Ju, F. Yang, X. Luo, L. Zhang, Uptake of methylene blue on divinylbenzene cross-linked chitosan/maleic anhydride polymer by adsorption process, Colloids Surf. A Physicochem. Eng. Asp. 629 (2021) 127424.

[28] F.I. El-Dib, G. Eshaq, A.E. ElMetwally, H.H.H. Hefni, Enhancing the porous structure of swellable poly(acrylic acid-co-acrylamide) crosslinked by N-Maleyl chitosan via introducing foaming agents and non-ionic surfactant, Adv. Ind. Eng. Polym. Res. 4 (2021) 9–18.

[29] F. Han, Y. Dong, Z. Su, R. Yin, A. Song, S. Li, Preparation, characteristics and assessment of a novel gelatin-chitosan sponge scaffold as skin tissue engineering material, Int. J. Pharm. 476 (2014) 124–133.

[30] J. Galan, J. Trilleras, P.A. Zapata, V.A. Arana, C.D. Grande-Tovar, Optimization of chitosan glutaraldehyde-crosslinked beads for reactive blue 4 anionic dye removal using a surface response methodology, Life 11 (2021) 85.

[31] M. Kim, H. Kim, Y.-S. Lee, S. Lee, S.-E. Kim, U.-J. Lee, S. Jung, C.-G. Park, J. Hong, J. Doh, D.Y. Lee, B.-G. Kim, N.S. Hwang, Novel enzymatic cross-linking–based hydrogel nanofilm caging system on pancreatic β cell spheroid for long-term blood glucose regulation, Sci. Adv. (2021). Jun23, eabf7832 (13 pages).

[32] V.R. Shaumbwa, D. Liu, B. Archer, J. Li, F. Su, Preparation and application of magnetic chitosan in environmental remediation and other fields: a review, J. Appl. Polym. Sci. 138 (2021) e51241.

[33] Y. Wang, M. Yang, J. Qian, W. Xu, J. Wang, G. Hou, L. Ji, A. Suo, Sequentially self-assembled polysaccharide-based nanocomplexes for combined chemotherapy and photodynamic therapy of breast cancer, Carbohydr. Polym. 203 (2019) 203–213.

[34] F. Doustdar, A. Olad, M. Ghorbani, Development of a novel reinforced scaffold based on chitosan/cellulose nanocrystals/halloysite nanotubes for curcumin delivery, Carbohydr. Polym. 282 (2022) 119127.

[35] J. Jirawutthiwongchai, A. Krause, G. Draeger, S. Chirachanchai, Chitosan-oxanorbornadiene: a convenient chitosan derivative for Click Chemistry without metal catalyst problem, ACS Macro Lett. 2 (2013) 177–180.

[36] R. Fagundes Correa, G. Colucci, N. Halla, J.-A. Pinto, A. Santamaría-Echart, S. P. Blanco, I.P. Fernandes, M.F. Barreiro, Development of chitosan microspheres through a green dual crosslinking strategy based on tripolyphosphate and vanillin, Molecules 26 (2021) 2325.

[37] M. Elhag, H.E. Abdelwahab, M.A. Mostafa, G.A. Yacout, A.Z. Nasr, P. Dambruoso, M.M. El Sadek, One pot synthesis of new cross-linked chitosan-Schiff` base: characterization, and anti-proliferative activities, Int. J. Biol. Macromol. 184 (2021) 558–565.

[38] J. Hu, Z. Wang, J.M. Miszuk, M. Zhu, T.I. Lansakara, A.V. Tivanski, J.A. Banas, H. Sun, Vanillin-bioglass cross-linked 3D porous chitosan scaffolds with strong osteopromotive and antibacterial abilities for bone tissue engineering, Carbohydr. Polym. 271 (2021) 118440.

[39] G. Martínez-Mejía, N.A. Vázquez-Torres, A. Castell-Rodríguez, J.M. del Río, M. Corea, R. Jiménez-Juárez, Synthesis of new chitosan-glutaraldehyde scaffolds for tissue engineering using Schiff reactions, Colloids Surf., A 479 (2019) 123658 (15 pages).

[40] P. Morales, E. Ramírez-Moreno, M.C. Sanchez-Mata, A.M. Carvalho, I.C.F. R. Ferreira, Nutritional and antioxidant properties of pulp and seeds of two xoconostle cultivars (Opuntia joconostle F.A.C. Weber ex Diguet and Opuntia matudae Scheinvar) of high consumption in Mexico, Food Res. Int. 46 (2012) 279–285.
[41] E. Valadez-Moctezuma, Q. Ortiz-Vázquez, S. Samah, Molecular based assessment of genetic diversity of xoconostle accessions (Opuntia spp.), Afr. J. Biotechnol. 13 (2014) 202–210.
[42] P. Morales, E. Ramírez-Moreno, M.C. Sanchez-Mata, A.M. Carvalho, I.C.F. R. Ferreira, Nutritional and antioxidant properties of pulp and seeds of two xoconostle cultivars (Opuntia joconostle F.A.C. Weber ex Diguet and Opuntia matudae Scheinvar) of high consumption in Mexico, Food Res. Int. 46 (2012) 279–285.
[43] A. El-Araby, L. El Ghadraoui, F. Errachidi, Physicochemical properties and functional characteristics of ecologically extracted shrimp chitosans with different organic acids during demineralization step, Molecules 28 (23) (2022) 8285, 27.
[44] L. Pérez, L. Ruiz, J.L. Vilas, Determining the deacetylation degree of chitosan: opportunities to learn instrumental techniques, J Chem. Educ. 95 (2018) 1022–1028.
[45] X.L. Tian, D.F. Tian, Y. Wang, F.K. Mo, Synthesis and evaluation of chitosan-vitamin C complex, Indian J. Pharmaceut. Sci. 71 (4) (2009) 371–376.
[46] A.K. Whitehead, H.H. Barnett, M.E. Caldorera-Moore, J.J. Newman, Poly(ethylene glycol) hydrogel elasticity influences human mesenchymal stem cell behavior, Regen. Biomater. 5 (2018) 167–175. Jun.
[47] Kamal Shah Reem, Mohamed Naglah Ahmed, Nanoarchitectonics of chitosan/glutaraldehyde/zinc oxide as a NovelComposite for the efficient removal of eriochrome black T dye from aqueous media, J. Inorg. Organomet. Polym. Mater. 32 (2022) 2030–2039.